Available online at www.sciencedirect.com
SCIENCE DIRECT
Journal of Sound and Vibration 295 (2006) 266–281
JOURNAL OF SOUND AND VIBRATION
www.elsevier.com/locate/jsvi

An analytical approach to wake interference effects on circular cylindrical structures

Rupert G. Williams[a,*], Wimal Suaris[b]

[a]National Housing Authority of the Republic of Trinidad and Tobago, 5, Fourth Street, Barataria, Trinidad and Tobago
[b]Civil Engineering at the University of Miami, Coral Gables, Florida, USA

Received 6 July 2004; received in revised form 30 June 2005; accepted 9 January 2006
Available online 2 May 2006

Abstract

When a body is immersed in the wake of another body the additional buffeting force due to the vortices shed from the upstream structure magnifies the amplitude of vibration of the downstream structure. The proposed semi-empirical model is of the coupled Rayleigh wake-oscillator type with the equation of motion including an additional buffeting force. For two structures consisting of different structural parameters and placed in tandem with a wind flow, the buffeting force experienced by the downstream structure can be extrapolated from the lift force of the upstream structure, by using the ratios of the Scruton number, for the two structures. The paper highlights the aerodynamic response of tandem structures in the three primary interference regions: the proximity interference region, where the separation of the structures lies between $1.0D$ and $1.1D$; the proximity induced galloping region where the separation lies between $1.1D$ and $3.8D$; and the wake interference region where the separation is greater than $3.8D$.

1. Introduction

When a body is immersed in the wake of another body the flow pattern gains in complexity, see Refs. [1–3]. This wake interference has many engineering applications, such as transmission lines, suspension bridges and offshore conductor pipes, the integrity of which is of major concern.

Through wind-tunnel experiments in the 1930s it was found that the torque on the Empire State Building in New York would be doubled if two building blocks were built on sites adjacent to it [4], indicating that the interference phenomenon should not be taken lightly. The collapse of the cooling towers at Ferrybridge, England in 1965 was considered to be the driving force behind the interference effect studies of that era. The studies began with simple exploratory tests that involved rigid building models and developed to the present with boundary layer investigations on building systems. The interference effect on large groups of buildings was also the focus of several investigations including Blessmann and Riera [5], and Melbourne [6].

*Corresponding author. Tel.: +1 868 679 1945; fax: +1 868 625 3963.
E-mail address: servilus@yahoo.com (R.G. Williams).

0022-460X/$ - see front matter © 2006 Elsevier Ltd. All rights reserved.
doi:10.1016/j.jsv.2006.01.023

Nomenclature

A	$x_{\max}$ (maximum lift amplitude of cylinder)
A_T	amplitude of vibration in lift direction
A_L	amplitude of vibration in streamwise direction
a	shortest distance between cylinders
a	$\rho D^2 l/(8\pi^2 S^2 M)$
b	constant value
C_D	drag coefficient
C_L	lift coefficient of body
c_L	instantaneous lift coefficient in τ domain
D	diameter of cylinder
F_L	lift force
$f(x)$	forcing function
$f(c_L)$	forcing lift force
f_s	frequency of vortex shedding, SV/D
f_n	fundamental frequency of body
L	along wind separation of cylinders
L	length of cylinder
m	mass per unit length of cylinder
Re	Reynolds number
S	Strouhal number
Sr	Scruton number, $m\zeta/(\rho D^2)$
T	across wind separation of cylinders
V	fluid stream velocity
v	wind velocity
V_r	reduced velocity, $V/(f_n D)$
V_{air}	volume of air
X_{max}	maximum dimensionless amplitude of lift displacement, x_{r-max}
$\boldsymbol{x}$	streamwise separation of cylinders
x	lift displacement
x_r	dimensionless lift displacement variable, x/D
$\boldsymbol{y}$	cross stream separation of cylinders
y	amplitude of vibration (lift direction)

Greek letters

α	damping constant in Rayleigh equation
ζ	damping ratio of cylinder, $C/(2M\omega_n)$
ζ_1	$C_1/(2M_1\omega_{n1})$
ζ'_2	$C_2/(2M_2\omega_{n2})$
ζ_2	$C_2/(2M_2\omega_{n1})$
δ	phase shift
ε	weighted constant for forcing function that depends on the value $(4M/L)/(\pi\rho_{\text{air}} DL)$
ε_0	Proportionality constant
ε_1	constant related to mass of cylinder
ε_2	constant related to mass of fluid medium
$\hat{\varepsilon}_1$	constant related to mass of cylinder 1
$\hat{\varepsilon}_2$	constant related to mass of cylinder 2
γ	damping constant
λ	separation variable for buffeting force
ω_0	f_s/f_n
ω_{01}	f_{s1}/f_{n1}
ω_{02}	f_{s2}/f_{n1}
ω_n	natural circular frequency of body, $2\pi f_n$
ω_s	strouhal circular frequency, $2\pi f_2$
ρ	density of fluid medium
τ_1	$L\omega_{n1}/V$
τ	$\omega_{n1} t$
$(\dot{})$	first-order derivative with respect to τ, $\mathrm{d}/\mathrm{d}\tau$
$(\,)'$	material time derivative, $\mathrm{d}/\mathrm{d}t$
$(\,)''$	second-order derivative, $\mathrm{d}^2/\mathrm{d}t^2$

The interference effect between two or more high-rise buildings may decrease or increase the static wind load but increase the dynamic response in most cases. Melbourne [6] writes that the dynamic response of a tall building in the wake of another may increase up to 100% and that the hourly maximum cross-wind base overturning moment may increase up to 40%. The dynamic influence caused by the increase of the turbulence within the wake of the upstream building continues for a fair distance downstream. Studies by Blessmann [5] on square prisms indicate that the torsional moment increases by more than three times the value measured on an isolated model. Zdravkovich [7] gives an overview of the regions of flow interference for two parallel circular cylinders shown in Fig. 1, where "y" is the cross-stream separation and "x" is the streamwise separation of the cylinders of diameter, D. The "wake interference" region is where one cylinder is partly or wholly immersed in the wake of the other. The "proximity interference" region is where the cylinders are not in or near the wake of their neighbor. For the tandem arrangement this is the region where the separation ratio ranges from 1.0 to 1.1. The region where the interference effects are combined in the side-by-side arrangement is the overlapping region. Outside of these regions the cylinders behave as isolated structures.

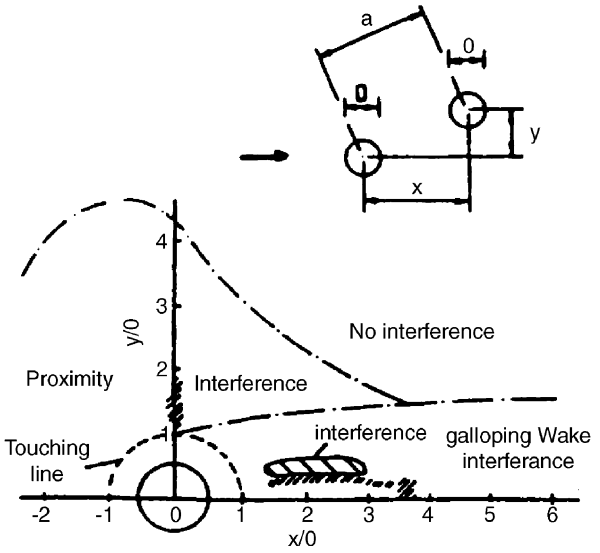

Fig. 1. Flow regimes for different arrangements of parallel circular cylinders. Source: Zdravkovich [7].

2. Previous research

2.1. Experimental

Published studies on the interference phenomenon have been mostly empirical. In these studies, the range of values of the Reynolds number at which the tests were conducted are outside actual values found in practice, making it difficult to extrapolate the results. For the two-dimensional case, the possible interference conditions that may arise between bodies of different shape or dimension are also innumerable. For example, at low Reynolds number, vortex shedding from a circular cylinder was controlled and suppressed by the placement of a second, much smaller cylinder in the near wake. The spatial region where the control cylinder should be placed to achieve suppression of vortex shedding is finite, and a function of its diameter. From works carried out by Ohya et al. [8], this region lies between $1.0D$ and $1.1D$ for the tandem arrangement of cylinders. This observation indicates that the secondary cylinder may have the effect of altering the local stability characteristics of the near wake [9].

The fluctuating components, i.e. the vortices shed from the upstream cylinder and the reduced mean velocity of the wake flow impinging on the downstream body, are parts of the rationale used to conclude that a cylinder located in the wake of another will not behave as an isolated one. The experimental results of Ohya et al. [8] for two stationary cylinders (in line) support this view; the aerodynamic parameters such as the drag and the lift forces, the pressure distribution, the Strouhal number and the vortex-shedding patterns differ significantly and depend strongly on the spacing L, between the centers of the cylinders (see Fig. 2.).

The tandem arrangement of cylinders, i.e. one cylinder placed behind the other, is characterized by the existence of a critical distance, $L_c \approx 3.8D$ below which the regular vortex shedding from the front cylinder is suppressed. For smaller values of L, different configurations may occur depending on the behavior of the shear layers separating from the front cylinder, which may or not reattach steadily or intermittently to the sides of the downstream cylinder [7]. For cylinders almost in contact, $(1 < L/D < 1.2 - 1.8)$ depending on the Reynolds number, they behave like a single elongated body, and the shear layers from the front cylinder do not reattach on the downstream one. As the boundary layer separation points are not fixed by geometry, the boundaries between the various regimes may depend on Reynolds number, turbulence and roughness [10,11].

As the distance between the cylinders is increased beyond the critical distance, L_c, the downstream structure experiences a buffeting force from the upstream structure. However, the buffeting force reduces as the separation is increased. Brika and Laneville [12] showed that as the separation of the structures approaches $10D$, the buffeting effect is negligible.

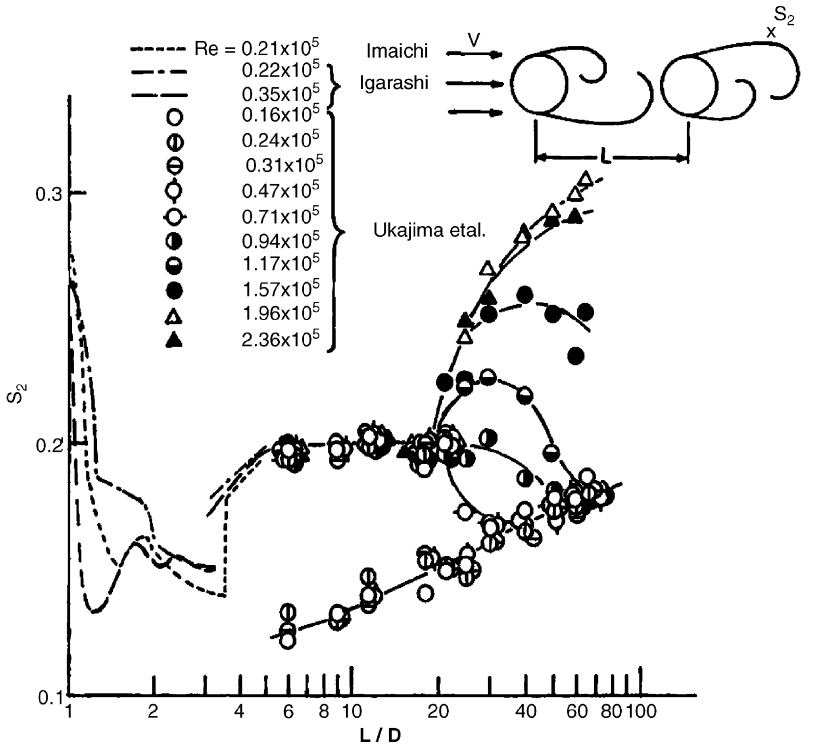

Fig. 2. Strouhal numbers behind a downstream cylinder. Source: Ohya et al. [8].

It is important to note that in many of the situations where slender structures are positioned next to similar structures, the asymmetries that may originate in the flow, even in symmetrical conditions, may produce mean cross-wind forces of a magnitude considerably greater than that experienced by an isolated structure. Therefore analytical models need to be developed that can model wake interference.

2.2. Analytical

The interference model by Shiau and Yang [13], which is an extension of the Hartlen and Currie [14] model, considers the wake interference region of identical structures. For two cylinders in tandem, their model was based on the following assumptions: (1) the distance between the cylinders is large enough so that the effect of the rear cylinder motion on the front cylinder can be neglected; (2) the vortex created by the motion of the front cylinder, after it reaches the second cylinder, acts as a buffeting force on the second cylinder. This vortex loses its effect as far as the wake behind the second cylinder is concerned.

The downstream cylinder is therefore subjected to two forces, the force on the cylinder due to its own vortex street, and the second force, the buffeting force from the wake of the upstream cylinder with a time delay to account for the separation of the two cylinders. It is to be noted here that their model was developed for two identical cylinders in tandem. Shiau and Yang [13] have not considered the separation effects of the additional buffeting force on the leeward cylinder. This leads to an overestimation of the response of the downstream cylinder.

In experiments conducted on cylinders by Bishop and Hassan [15] it was observed that the lift force acting on a system is a function of the amplitude of vibration, and this lift force is a self-excited oscillatory mechanism in the flow field. This observation is an important factor in the present paper. The most successful model to date for estimating the lift force on cylinders is that of Hartlen and Currie [14] where a Van de Pol representation is considered for the oscillating lift force. The limitation of this model lies in the choice of the forcing term in the aerodynamic equation, where a secular term was used. The incompleteness of the term may

lead to divergent oscillations and eventually instability in the system equations. The other main drawback of their model is the relating of the parameters, α and γ to the initial lift coefficient, c_{L0}. Based on a parametric study, the limit cycle of the aerodynamic equation was found to be independent of c_{L0}, and solely dependent on α and γ. Therefore, the Hartlen and Currie relationship linking α and γ to c_{L0} appears to be invalid. Coupling this equation to the equation of motion and choosing the parameters appropriately, Shiau and Yang [13] was able to qualitatively reproduce the behavior of the downstream cylinder, i.e. the important synchronization phenomenon along with limiting peak response amplitude at the end of synchronization. The model developed in this paper considers two cylinders with different structural parameters and the effect of separation on the wake interference is also addressed.

The advances in the field of computational fluid dynamics due mainly to the use of the finite element technique have produced many papers on the topic of vortex-induced vibration. Some include the works of Normura and Hughes [16], Normura [17] and Dipankar and Sengupta [18].

The systems developed by Normura [17] and Dipankar and Sengupta [18] focused basically on isolated bodies. The modeling of a mixed vortex pattern between two bodies that posses independent degrees of freedom was not been attempted. Although great strides have been made in the field of CFD, the interference phenomenon is yet to be challenged by way of discretization models.

3. Proposed model

3.1. Wake oscillator model for isolated cylinder

Considering the equation of motion in its fundamental form, we have the following:

$$x'' + \text{Damping Term} + \omega_n^2 x = \varepsilon_1 f(c_L), \tag{1}$$

where x is the displacement in the lift direction, $f(c_L)$ is a forcing function related to the lift (wind) coefficient, c_L and ε_1 is a constant related to the mass of the cylinder, with ω_n being the natural frequency of the cylinder. The prime denotes differentiation with respect to time, t.

Introducing the lift force function $f(c_L)$ as a product of the static pressure and the cross-sectional area of the cylinder, i.e. $\frac{1}{2}\rho v^2 DLc_L$ and $\varepsilon_1 = 1/M$, the equation becomes

$$x'' + \text{Damping Term} + \omega_n^2 x = \frac{1}{M} DL\tfrac{1}{2}\rho v^2.c_L, \tag{2}$$

where M is the mass of the cylinder of diameter D, and length L. ρ is the density of the fluid medium, v is the velocity of the fluid stream and c_L is the lift (wind) coefficient with ω_n being the natural frequency of the cylinder.

The aerodynamic equation can be written in a similar form as:

$$c_L'' + \text{Damping Term} + \omega_s^2 c_L = \varepsilon_2 \frac{f(x)}{L}, \tag{3}$$

where $f(x)/L$ is a forcing function per unit length related to the motion of the cylinder. This forcing function is given per unit length to be consistent with the forcing function in the equation of motion and also for the equation to be dimensionally consistent. By analogy with Eq. (1), ε_2 is a function of the wind mass, represented by $\rho_{\text{air}} V_{\text{air}}$, the product of the density of the fluid medium and the contributing volume of air. $\omega_s = 2\pi f_s$ the Strouhal circular frequency.

From preliminary analyses, using a series expression for the forcing function, the lift coefficient c_L was observed to be proportional to the amplitude of vibration, before and up to the end of the synchronization region. This behavior is consistent with the results of the experiments of Bishop and Hassan [15].

Introducing $\tau = \omega_n t$ and noting that

$$\frac{\mathrm{d}^2 c_L}{\mathrm{d}t^2} = \omega_n^2 \frac{\mathrm{d}^2 c_L}{\mathrm{d}\tau^2}, \quad \frac{\mathrm{d}^2 x_r}{\mathrm{d}t^2} = \omega_n^2 \frac{\mathrm{d}^2 x_r}{\mathrm{d}\tau^2},$$

Eqs. (1) and (3) can be written using dimensionless parameters in the τ domain as

$$\ddot{x}_r + \text{Damping Term} + x_r = \frac{1}{M} L \frac{\frac{1}{2}\rho v^2 c_L}{\omega_n^2}, \tag{4}$$

$$\ddot{c}_L + \text{Damping Term} + \omega_0^2 c_L = \varepsilon_2 \frac{f(x_r) D}{\omega_n^2 L}, \tag{5}$$

where x_r is the dimensionless lift displacement x/D and $\omega_0^2 = \omega_s^2/\omega_n^2$.

A recurrence relation may be set up for $f(x_r)$ as

$$f(x_r) = k_c(x_r + \Delta\tau \dot{x}_r), \tag{6}$$

where k_c is the stiffness of the cylinder in the lift direction. This form is chosen since x_r is the lift displacement; therefore, the lift force is a product of this "displacement" and the corresponding stiffness.

Now recalling that k_c/ω_n^2 is the mass (M) of the cylinder and assuming the contributing volume of air is proportional to the volume of the cylinder, Eq. (5) can be written in a dimensionally consistent form as

$$\ddot{c}_L + \text{Damping Term} + \omega_0^2 c_L = \varepsilon_0 \frac{4M}{\pi \rho_{\text{air}} D L^2}(x_r + \Delta\tau \dot{x}_r), \tag{7}$$

where the term ε_0 is a proportionality constant since the contributory volume of air was assumed to be proportional to the cylinder's volume. The parameter ε_0 in Eq. (7) was introduced to validate the assumption that the contributory volume of air was proportional to the cylinder's volume. Physically we know from historical perspectives that structures with larger inertia require a larger wind velocity (lift force) to produce motion. And for similar structures of the same material, the inertia is related to the volume of the structure. Therefore, the "inertia force" is related to the structures volume. It should be noted that the constant term on the right-hand side of Eq. (7) bears a similarity to Scruton's number except the damping ratio.

The two equations given below are chosen to represent the isolated system. They are the general second-order equation of motion and the modified Rayleigh equation. These equations are similar to the system of equations developed by Hartlen and Currie [14], with the exception of the forcing term in the aerodynamic equation being modified:

$$\ddot{x}_r + 2\zeta \dot{x}_r + x_r = a\omega_0^2 c_L, \tag{8}$$

$$\ddot{c}_L - \alpha\omega_0 \dot{c}_L + \frac{\gamma}{\omega_0}\dot{c}_L^3 + \omega_0^2 c_L = \varepsilon_0 \frac{4M}{\pi \rho_{\text{air}} D L^2}.(x_r + \Delta\tau \dot{x}_r). \tag{9}$$

The parameters, α and γ are damping terms, with α being a negative damping term and γ, a positive damping term. The forcing function of the aerodynamic equation (9) is related to the motion of the cylinder. The constant $a = \rho D^2 L/(8\pi^2 S^2 M)$ where S is the Strouhal number.

The damping function in the aerodynamic equation (9) is used in preference to the classical Rayleigh equation since the limit cycle in this form is independent of the reduced velocity, ω_0 whereas the classical model shows some dependence on the reduced velocity. The classical form also has one damping constant whereas the form chosen here has two damping terms, which gives greater flexibility in the evaluation of the parameters to match the various experimental data.

The method used for the solution of the system of equations was the finite difference approximation. Initially a parametric study was carried out on the Rayleigh equation using the Euler method. From this analysis the limit cycle was found to be independent of the initial conditions c_{L0} and dependent solely on α and γ. In applying the finite difference approximation to the solution of the system equations (8) and (9), the values for x_{-1} and $\ddot{x}_0$ were generated from recurrence relationships. A Fortran 90 compiler was utilized to generate the algorithms. The time step used, along with the precision of the compiler eliminated the presence of nonlinear instability due to manipulation of small numbers.

3.2. Calibration of the model parameters

The experimental works of Brika and Laneville [12] and Goswami et al. [19], were used to evaluate the parameters α and γ. Expressing Eq. (9) in a form that is numerically manageable, the constant term ε_0 is chosen so as to make the coefficient unity for the Goswami's experimental series. The numerical value of ε_0 is chosen so as to be consistent with the expected magnitude of the structure's displacement. The values for all the other tests were pro-rated in accordance with their respective values of the term $4M/L/(\pi\rho_{\text{air}}DL)$.

The terms α and γ are damping terms, with α being a negative damping term that affects the location of the maximum amplitude and γ a positive damping term. Both these terms were taken as being related to Scruton's number ($Sr\#$), which is related to the damping ratio. The Scrutons number was chosen in preference to the damping ratio since its value provides greater flexibility as its size is numerically manageable.

Once the values of the parameters were identified for the relevant experiments a simple regression analysis was carried out using the Scrutons number as the independent variable.

From this analysis the parameters α and γ were established as

$$\alpha = 2.13\mathrm{e}^{-Sr\#}, \tag{10}$$

$$\gamma = 0.0136\mathrm{e}^{Sr\#} + 0.36. \tag{11}$$

Figs. 3 and 4 show the results of the analytical model compared with the experimental results of Goswami [19] for two damping ratios.

3.3. Wake oscillator interference model

The proposed interference model is based on a tandem arrangement of two structures. Three separate regions are considered based on the experimental evidence that show distinct vortex shedding patterns. The flow patterns vary producing various aerodynamic characteristics depending on the separation distance for the tandem arrangement of cylinders. Ishigai et al. examined the flow pattern around two cylinders (taken from Ref. [8]). They found that below a critical spacing L/D of 3.8, regular velocity fluctuation was observed only behind the downstream cylinder. For spacing ratios greater than 3.8, vortex streets formed behind both cylinders and the values of the vortex shedding frequencies were the same. For spacing ratios less than 1.1 the vortex pattern was identical to that of a single elongated body (see Fig. 5).

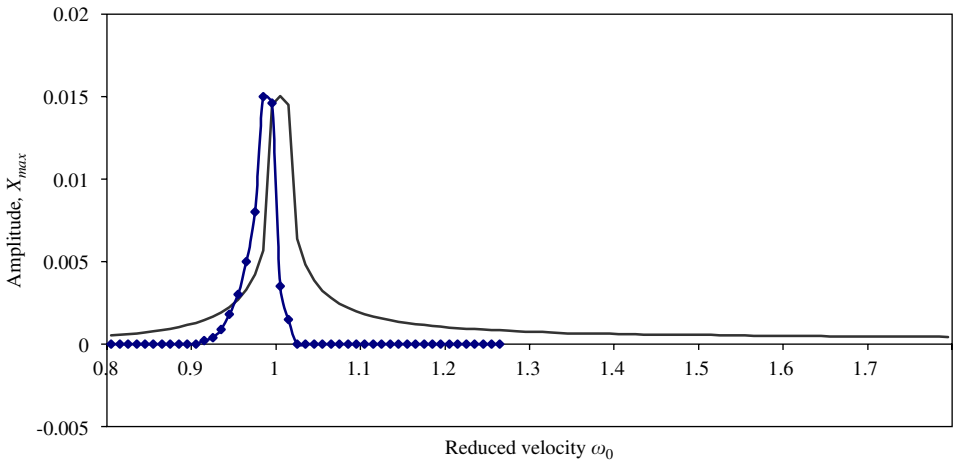

Fig. 3. Response amplitude for analytical and empirical model, Goswami et al. ($X_{\max}$ versus ω_0): ———, $\zeta = 0.301\%$—analytical; ——▶——, $\zeta = 0.301\%$—experimental.

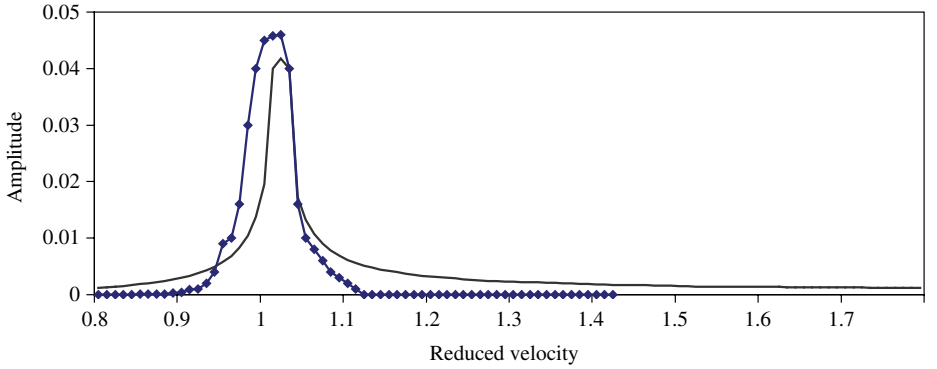

Fig. 4. Response amplitude for analytical and empirical model, Goswami et al. (X_{max} versus ω_0). ———, $\zeta = 0.149\%$—analytical; ——▶——, $\zeta = 0.149\%$—experimental.

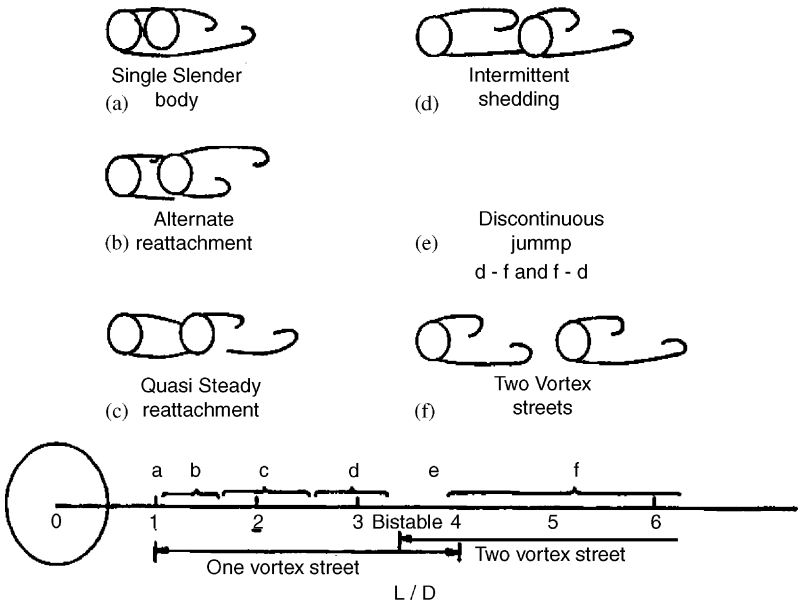

Fig. 5. Classification of flow regimes in tandem arrangements. Source: Zdravkovich [7].

3.4. Wake oscillator interference model: proximity interference ($L/D < 1.1$)

For a spacing ratio L/D less than 1.1 the two cylinders behave as one long slender body with a high Strouhal number. The separated shear layers formed behind the upstream cylinder are not able to reattach behind the downstream cylinder. The flow between the two cylinders is basically still, with vortices forming only behind the downstream cylinder. The typical flow pattern in this region is shown in Fig. 5(a).

As no vortices are shed from the upstream cylinder and as the flow between the two cylinders are basically stagnant, we can assume the lift response of the windward cylinder is negligible.

The response pattern of the downstream cylinder is more complex than that of the upstream cylinder. Initially vortices are shed from this cylinder at a high Strouhal number and then, as the separation ratio increases beyond 1.0 and approaches 1.1 the Strouhal number have been observed to decrease rapidly (see Fig. 2).

For this region, the Strouhal number of the downstream cylinder can be approximated by the equation

$$S = 0.67e^{-(L/D_1)^2}, \tag{12}$$

where D_1 is the diameter of the upstream cylinder and L is the separation between the cylinders.

The graph in Fig. 6 shows the vortex shedding frequency versus the velocity relationship according to Strouhal. As the velocity increases, the frequency increases until the natural frequency of the structure is reached and then lock-in begins at this constant frequency. After a certain increase in velocity, the system comes out of lock-in and continues at the frequency corresponding to the exit velocity based on the same Strouhal frequency relationship.

From Fig. 6, we see that for a given cylinder, as the Strouhal number decreases, the velocity at which synchronization begins increases. Therefore as the Strouhal number reduces, there is a lag in the system. As the spacing ratio, L/D increases, in the proximity interference region, the Strouhal number of the downstream cylinder reduces and thus causes an increase in velocity at which synchronization begins.

Therefore, the shift in the synchronization velocities for the two Strouhal numbers S_1 and S_2 can be expressed as

$$V_2 - V_1 = D_1 f_n \left(\frac{1}{S_2} - \frac{1}{S_1} \right). \tag{13}$$

We may assume that the synchronization range is the same at all values of Strouhal number. This assumption is based on the observation that the synchronization range is independent of the magnitude of the Strouhal frequency (see Fig. 6). The results of Goswami et al. [19] indicate that the response amplitude is related to the Scruton number (see Fig. 7). We can therefore assume that the response amplitude of the cylinder is independent of the value of the Strouhal number.

Fig. 8 shows the response amplitude of the downstream cylinder obtained using the test parameters for the Brika and Laneville [12] tests. The modified velocity is defined as $V/f_n D$ which is the same as the reduced velocity as defined by Brika and Laneville [12]. The Strouhal number for the downstream cylinder for the case of two cylinders in tandem in the above region ranges from 0.25 to 0.15. And since the Strouhal number of an isolated cylinder, in the sub-critical region of Reynolds number has a constant value of 0.2, the response curve for the downstream cylinder in the proximity region can be extrapolated from the response curve of the isolated cylinder case.

3.5. Wake oscillator interference model: wake interference ($L/D > 3.8$)

In this range of L/D greater than the limiting value of 3.8, the shear layers from the upstream cylinder roll up and form vortices (see Fig. 5). Therefore, two vortex streets are formed behind each cylinder. The results of

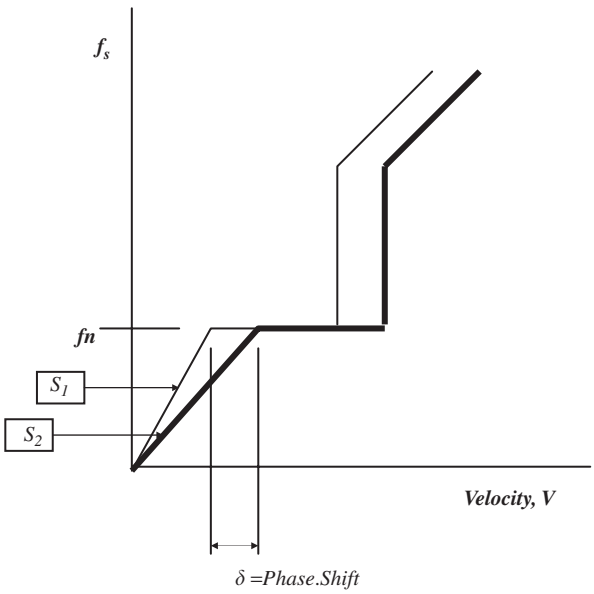

Fig. 6. Variation of Strouhal frequency Versus velocity V ($f_s = S.V/D_1$): ———, S_2; ———, S_1.

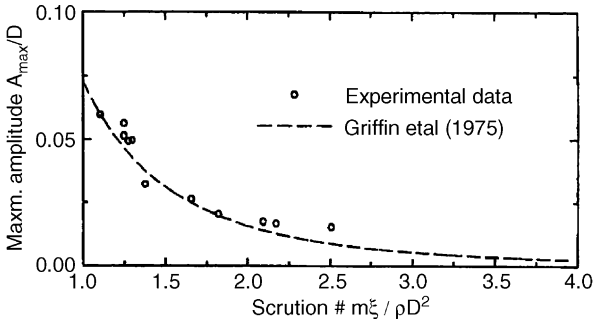

Fig. 7. Maximum amplitude, X_{max} versus Scruton number. Source: Goswami et al. [19].

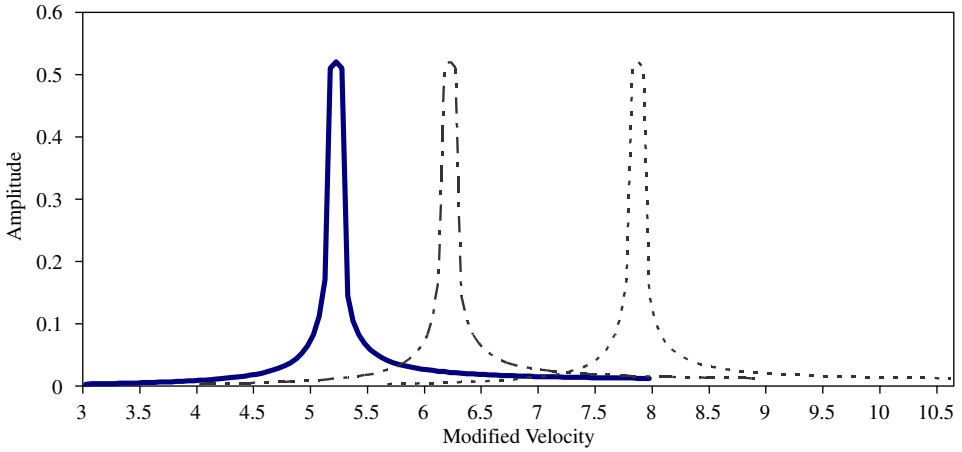

Fig. 8. Proximity interference response of leeward cylinder; Brika and Laneville model [12] (X_{max} versus V/f_nD): ———, $S = 0.25$, $L/D = 1.0$; – · – · – ·, $S = 0.2$, $L/D = 1.07$; – – –, $S = 0.15$, $L/D = 1.1$.

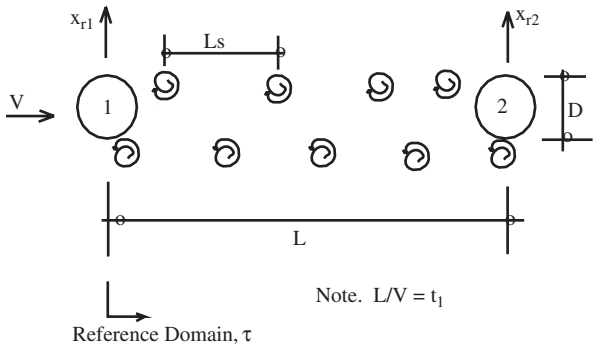

Fig. 9. Schematic diagram for two cylinders in tandem.

Brika and Laneville [12] indicate that the response amplitude of the downstream cylinder in a tandem arrangement approached that of the upstream cylinder for a separation ratio of 10 i.e. negligible interference effects.

Tests by Brika and Laneville [12] and Gowda et al. [20] have shown that the response of the upstream cylinder can be assumed to be the same as for an isolated cylinder for $L/D > 3.8$.

The effect of the motion of the downstream cylinder (cylinder 2) on the upstream cylinder (cylinder 1) can therefore be neglected and the equations for cylinder one in the τ domain can be written as, using

Eqs. (8) and (9) (see Fig. 9)

$$\ddot{x}_{r1} + 2\zeta_1 \dot{x}_{r1} + x_{r1} = a_1 \omega_{01}^2 c_{L1}, \tag{14}$$

$$\ddot{c}_{L1} - \alpha_1 \omega_{01} \dot{c}_{L1} + \frac{\gamma_1}{\omega_{01}} (\dot{c}_{L1})^3 + \omega_{01}^2 c_{L1} = \hat{\varepsilon}_1 (x_{r1} + \Delta\tau \dot{x}_{r1}). \tag{15}$$

The subscript 1 indicate that the parameters used are for the windward cylinder (cylinder 1).

The following assumptions are made for predicting the behavior of the leeward cylinder: (1) the buffeting force on the leeward cylinder due to the windward cylinder loses its effect as far as the wake behind the leeward cylinder is concerned; (2) the buffeting force from the windward cylinder and the lift force due to the leeward cylinder itself act together upon the leeward cylinder; and (3) the buffeting force on the leeward cylinder is inversely proportional to the Scruton number, $Sr = m\zeta/(\rho D^2)$, which is based on the results of Griffin et al. (see Fig. 7).

Incorporating the above assumptions, the equation of motion for the leeward cylinder may be written in the reference time domain ($\tau = \omega_{n1} t$) as

$$\ddot{x}_{r2} + 2\zeta_2 \dot{x}_{r2} + \frac{\omega_{n2}^2}{\omega_{n1}^2} x_{r2} = a_2 \omega_{02}^2 c_{L2} + \left(\frac{Sr_1}{Sr_2}\right) \frac{D_1}{D_2} \frac{M_1}{M_2} a_1 \omega_{01}^2 c_{L1}(\tau - \tau_1)\lambda, \tag{16}$$

where the parameter λ accounts for the effect of the spacing of the two cylinders on the buffeting force. Its development will be addressed subsequently.

$$\tau_1 = L\omega_{n1}/V.$$

The subscript 2 indicates that the parameters used are for cylinder 2.

The parameters used are defined as follows:

$$a_1 = \frac{\rho D_1^2 L}{8\pi^2 S_1^2 M_1}, \tag{17}$$

$$\zeta_2 = \frac{C_2}{2M_2 \omega_{n1}}, \tag{18}$$

$$\omega_{02} = \frac{f_{s2}}{f_{n1}} = \frac{S_2 V}{D_2 f_{n1}}, \tag{19}$$

$$Sr_1 = \frac{m_1 \zeta_1}{\rho D^2}. \tag{20}$$

And similarly the expression for Sr_2 can be obtained.

For the aerodynamic equation, if we consider the variable, τ_2 such that

$$\tau_2 = \frac{\omega_{n2}}{\omega_{n1}} \tau \tag{21}$$

and using the same reference domain we have

$$\ddot{c}_{L2} \frac{\omega_{n1}^2}{\omega_{n2}^2} - \alpha_2 \hat{\omega}_{02} \dot{c}_{L2} \frac{\omega_{n1}}{\omega_{n2}} + \frac{\gamma_2}{\hat{\omega}_{02}} \left(\dot{c}_{L2} \frac{\omega_{n1}}{\omega_{n2}}\right)^3 + \hat{\omega}_{02}^2 c_{L2} = \hat{\varepsilon}_2 \left(x_{r2} + \Delta\bar{\tau} \dot{x}_{r2} \frac{\omega_{n1}}{\omega_{n2}}\right). \tag{22}$$

The new parameter defined is

$$\hat{\omega}_{02} = \frac{f_{s2}}{f_{n2}} = \frac{S_2 V}{D_2 f_{n2}}. \tag{23}$$

Eqs. (14)–(16) and (22) represent the equations for the proposed interference model. All the variables considered are functions of τ, but in the use of the equations to evaluate the response of the leeward cylinder, the time domain, τ is taken as greater than t_1. Therefore, the system of equations are nonlinear and are evaluated in the domain $\tau \geqslant t_1$ where t_1 takes the value $(d/V)\omega_{n1}$, and τ is equal to $\omega_{n1} t$ (see Fig. 9). The

proportionality constants $\hat{\varepsilon}_1$ and $\hat{\varepsilon}_2$ are based on the value of the expression $4M/(\pi\rho_{\text{air}}DL^2)$ for the respective cylinders.

The effect of the separation of the cylinders on the buffeting force is accounted for in the model by the use of the parameter λ (see Eq. (16)).

By examining the physical significance of λ, the limits of this parameter can be established. For the case of a separation ratio of 3.8, i.e. at the critical separation, the works of Zdravkovich [7] and also Vickery [21] indicates that the lift response of the downstream cylinder is largest, therefore, λ has to be unity for this case. This is also justified based on the works Melbourne [6] where the dynamic response of a structure in the wake of another is said to increase by up to 100%. For the other extreme case of the cylinders being at an infinite distance apart (which is considered to be equivalent to a spacing ratio of 10), the buffeting force is negligible, since the vortices from the windward or front cylinder would have mixed and dissipated sufficiently to have no effect. The experimental results of Brika and Laneville [12] show that at a separation of $10D$ the interference effect is almost negligible.

Considering the limits of the parameter as discussed above, the simplest form of expression is introduced for λ as

$$\lambda = \mathrm{e}^{-(L/D-3.8)}, \tag{24}$$

where L is the spacing between the centers of the cylinders and D is the diameter of the upstream cylinder. A simple plot of the expression is shown in Fig. 10.

Using the parameters developed for the isolated cylinder, the response of the windward and leeward cylinders was established for the wake interference zones. The analytical results for the leeward cylinder are shown in Fig. 11 for a range of L/D ratios.

The results of the model were matched with those of Brika and Laneville [12] and Zdravkovich [22]. The results are shown in Tables 1 and 2. The amplitude of the response is matched almost identically whereas the locations of the peaks are slightly offset indicating the parameters α and γ can still be refined. The model is therefore predicting with an acceptable level of accuracy the synchronization phenomenon both in magnitude and location.

3.6. Wake oscillator interference model: proximity galloping ($1.1 < L/D < 3.8$)

In the region where L/D is between 1.1 and 3.8 the shear layers from the upstream cylinder begin initially to reattach themselves to the front of the rear cylinder in phase with the vortex shedding frequency of the rear cylinder. As the spacing is increased however, the reattachment phase is mixed with alternate vortex shedding from the upstream cylinder. The downstream cylinder continues to shed vortices periodically (see Fig. 5(b)).

For the upstream cylinder, as the spacing ratio increases from 1.1 to 3.8, the Strouhal number is assumed to pass from a value of zero to 0.2, since in the initial stages there is no vortex shedding and as the spacing ratio

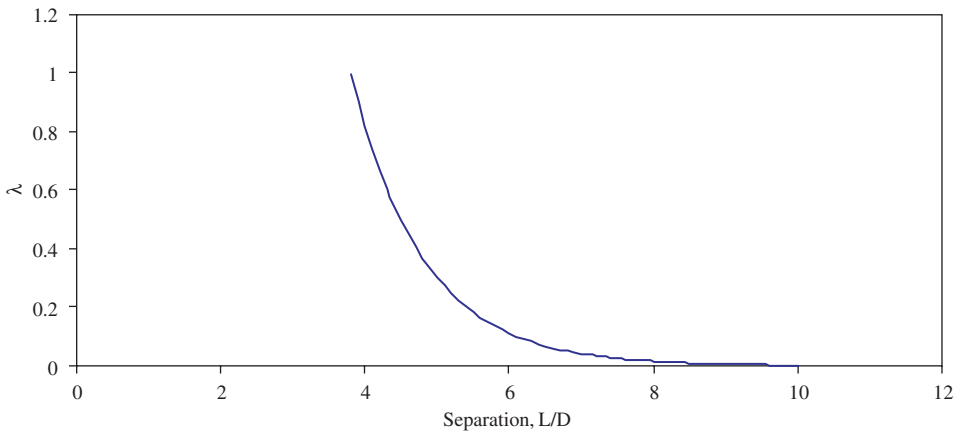

Fig. 10. Plot of λ versus separation ratio, $\lambda = \mathrm{e}^{-(L/D-3.8)}$.

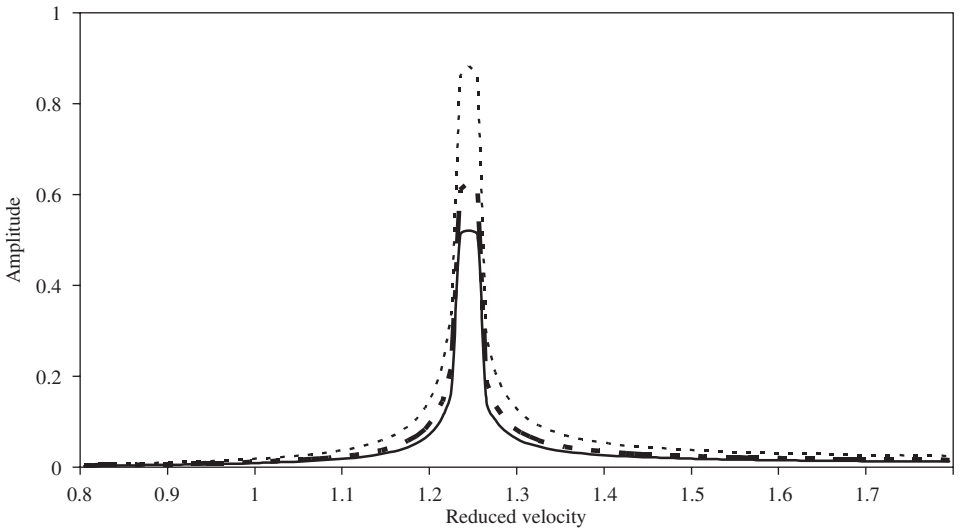

Fig. 11. Wake interference response of leeward cylinder at various separation ratios for $\zeta = 0.0083\%$; Brika and Laneville model [12]. (X_{max} versus ω_0): ———, $L/D = 10.0$; – · – $L/D = 5.0$; ....., $L/D = 3.8$.

Table 1
Response amplitudes for vortex shedding excitation of leeward cylinder-tandem positions (Zdravkovich)

L/D	Reduced lift amplitude—experimental A_T/D	Reduced velocity at maximum amplitude—experimental V/f_nD	Reduced lift amplitude—analytical model A_T/D	Modified velocity at maximum amplitude—analytical model V/f_nD
4.5	0.045	5.0	0.05	5.1
7.0	0.015	5.1	0.025	5.1

Table 2
Response amplitudes for vortex shedding excitation of cylinders-tandem positions (Brika and Laneville)

L/D	Reduced lift amplitude—experimental A_T/D	Reduced velocity at maximum amplitude—experimental V/f_nD	Reduced lift amplitude—analytical model A_T/D	Modified velocity at maximum amplitude—analytical model V/f_nD
10 (Windward)	0.51	6.2	0.5	6.15
10 (Leeward)	0.55	6.75	0.54	6.25

increases the shear layers roll up to form vortices which are shed. Fig. 12 shows a proposed frequency variation for the Strouhal number for the upstream cylinder in this region.

In the region where the Strouhal number is approximately zero the lift response will be zero. As the separation ratio increases, the Strouhal number increases and the cylinder begins to experience a lift response. The frequency of the response gradually increases until it reaches that of an isolated cylinder with a Strouhal number of 0.2. The amplitude of the response will be less than or equal to that of the isolated cylinder since the vortices are not shed at regular intervals and the shedding pattern is not fully developed.

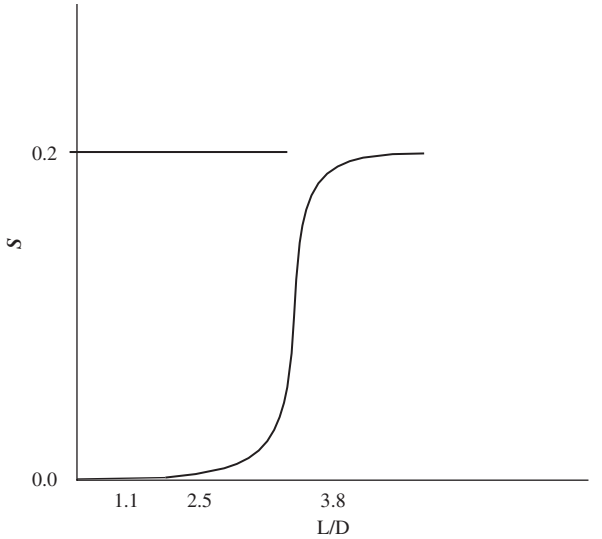

Fig. 12. Variation of Strouhal number for upstream cylinder in galloping region.

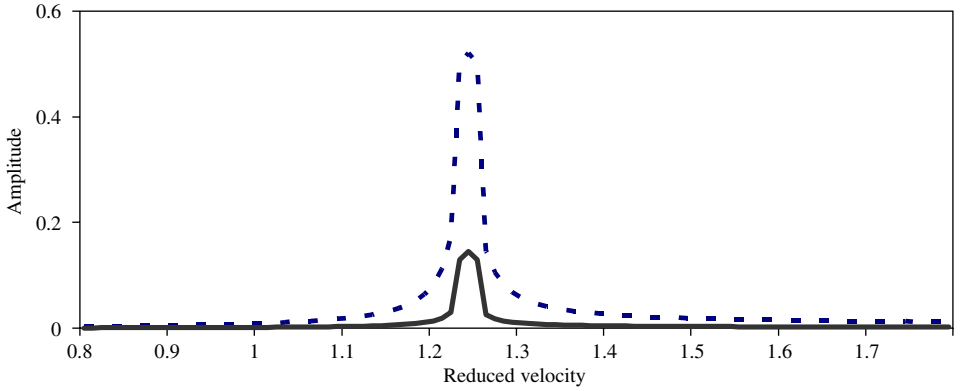

Fig. 13. Proximity galloping response for windward structure ($X_{\max}$ versus ω_0): – – – –, $L/D = 3.8$; ———, $L/D = 2.0$.

Therefore, suitable governing equations for the windward cylinder in this region can be introduced as

$$\ddot{x}_{r1} + 2\zeta_1 \dot{x}_{r1} + x_{r1} = a_1 \omega_{01}^2 c_{L1} e^{(L/D-3.8)}, \tag{25}$$

$$\ddot{c}_{L1} - \alpha_1 \omega_{01} \dot{c}_{L1} + \frac{\gamma_1}{\omega_{01}} (\dot{c}_{L1})^3 + \omega_{01}^2 c_{L1} = \hat{\varepsilon}_1 f(x_{r1}). \tag{26}$$

The factor $e^{(L/D-3.8)}$ accounts for the partial development of vortex shedding behind the windward cylinder. This expression is approximately zero for a spacing ratio of 1.1 and unity for a spacing ratio of 3.8. This is in accordance with the behavior of the cylinder, which experiences no vortex shedding, i.e. zero lift force for the spacing ratio of 1.1. As the vortex shedding develops and stabilizes at a Strouhal number of 0.2, i.e. at a spacing ratio of 3.8, the maximum lift response of the isolated cylinder is retrieved.

The equations developed in the previous section for wake interference are applicable for the response of the downstream cylinder in the proximity induced galloping region, i.e. Eqs. (16) and (22).

Figs. 13 and 14 show some predicted results in the galloping region for the Brika and Laneville series. The increase in amplitude with the increase in spacing can be observed for both the windward and leeward cylinders.

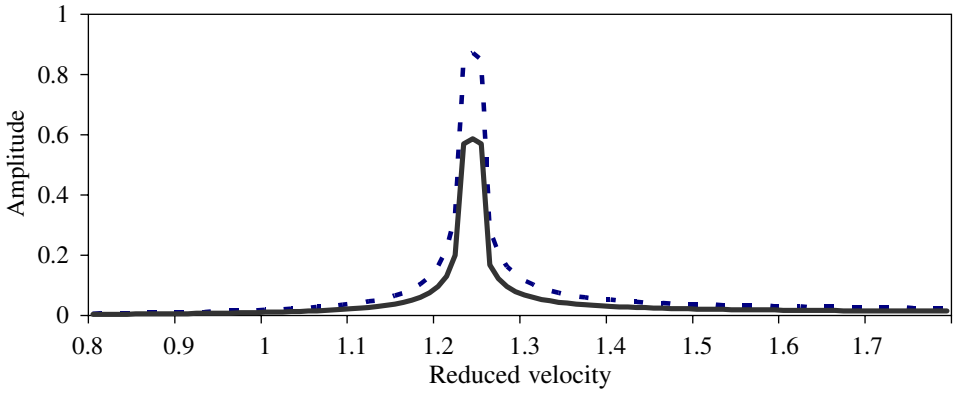

Fig. 14. Proximity galloping response for leeward structure (X_{max} versus ω_0): – – – –, $L/D = 3.8$; ———, $L/D = 2.0$.

4. Summary and conclusions

The general use of parameters directly related to the geometrical properties makes the model suitable for extrapolating the response of real structures of any shape and size and not just limited to cylindrical shapes.

The analytical model developed in the paper accurately predicted the results of the several experimental investigations. In the experimental work by Goswami [16], what is evident is that the reduced velocity at which the peak response occurs is reduced as the damping increases. This indicates that structures with higher damping are prone to respond at their critical amplitudes at lower wind velocities than structures with lower damping, but the magnitude of this amplitude remains lower as expected for the structures with higher damping.

The interference model developed in the paper considered three dominant regions: the proximity interference region, the induced galloping region and the wake interference region.

In employing the quasi-steady approach in the proximity interference zone as the separation increased from 1.0 to 1.1, a phase shift in the response of the downstream structure is predicted. Physically this is reasonable since the cylinders are so close that a substantial shielding effect occurs with the effect of the wind on the downstream cylinder being unaltered for the separation ratio between 1.0 and 1.1, therefore not affecting the amplitude of the response.

For the wake interference region, i.e. $L/D > 3.8$ the vortex pattern on the two cylinders becomes regularized and the vortex trail of the upstream cylinder "fuels" its wake and causes an increase in the vibration amplitude of the downstream cylinder. The interference effects are a maximum at $L/D \approx 3.8$ diminishing to almost zero as the separation reaches $10D$.

The model developed in the paper was found to be successful in reproducing the synchronization phenomenon in wake interference. The synchronization velocity and the peak amplitude were predicted well by the model.

The three major interference zones, determined by the separation between the windward and leeward structures, have been accounted for using available experimental results.

References

[1] M.M. Zdravkovich, Review of flow interference between two circular cylinders in various arrangements, *Journal of Fluids Engineering ASME* 99 (1977) 618–633.

[2] M.M. Zdravkovich, Review of interference-induced oscillations in flow past two parallel circular cylinders in various arrangements, *Journal of Wind Engineering and Industrial Aerodynamics* 28 (1988) 183–200.

[3] S.S. Chen, A review of flow-induced vibration of two circular cylinders in cross flow, *Journal of Pressure Vessel Technology ASME* 108 (1986) 382–393.

[4] A.C. Khanduri, T. Stathopoulos, C. Bédard, Wind-induced interference effects on buildings- a review of the state-of-the-art, *Engineering Structures* 20 (7) (1998) 617–630.
[5] J. Blessmann, J. D. Riera, Interaction effects in neighboring tall buildings, in: *Proceedings of the fifth International conference on Wind Engineering*, Vol. 1, Pergamon Press, Oxford, 1980, pp. 381–395.
[6] W. H. Melbourne, Cross-wind response of structures to wind action, in: *Proceedings of the fourth International Conference of Wind Effects on Buildings and Structures*, Cambridge University Press, London, 1975, pp. 343–358.
[7] M.M. Zdravkovich, The effects of interference between circular cylinders in cross flow, *Journal of Fluid and Structures* 1 (1987) 239–261.
[8] Y. Ohya, A. Okajima, and M. Hayashi, Wake interference and vortex shedding, in: N. Cheremisinoff (Ed.), *Encyclopedia of Fluid Mechanics*, Vol. 8, 1989, pp. 323–389.
[9] G. Buresti, Vortex shedding from bluff bodies, in: Proceedings of the Jubileum Conference on Wind Effects on Buildings and Structures. Brazil, May 1998, pp. 61–95.
[10] T. Igarashi, Characteristics of the flow around two circular cylinders arranged in tandem, *Bulletin JSME* 24 (1981) 323–331.
[11] H. Zhang, W.H. Melbourne, Interference between two circular cylinders in tandem in turbulent flow, *Journal of Wind Engineering and Industrial Aerodynamics* 41–44 (1992) 589–600.
[12] D. Brika, A. Laneville, Wake interference between two circular cylinders, *Journal of Wind Engineering and Industrial Aerodynamics* 72 (1997) 61–70.
[13] Le-Chung Shiau, T.Y. Yang, Two-cylinder model for wind vortex-induced vibration, *Journal of Engineering Mechanics* 113 (5) (1987) 780–789.
[14] R. T. Hartlen, Iain G. Currie, Lift-oscillator model of vortex-induced vibration, *Journal of the Engineering Mechanics Division*, ASCE 96 EM5 (1970) 577–591.
[15] R.E.D. Bishop, A.Y. Hassan, The lift and drag forces on a circular cylinder in a flowing fluid, *Proceedings of the Royal Society of London. Series A, Mathematical and Physical Sciences* 277 (1368) (1964) 32–50.
[16] T. Nomura, T.R. Hughes, An arbitrary Lagrangian–Eulerian finite element method for interaction of fluid and a rigid body, *Computer Methods in Applied Mechanics and Engineering* 95 (1992) 115–138.
[17] T. Nomura, A numerical study on vortex-excited oscillations of bluff cylinders, *Journal of Wind Engineering and Industrial Aerodynamics* 50 (1993) 75–84.
[18] A. Dipankar, T. Sengupta, Flow past a circular cylinders in the vicinity of a plane wall, *Journal of Fluids and Structures* 20 (3) (2005) 403–423.
[19] I. Goswami, R. Scanlan, N. Jones, Vortex-induced vibration of circular cylinders. I: experimental Data, *Journal of Engineering Mechanics* 119 (11) (1993) 2270–2287.
[20] L.B.H. Gowda, V. Sreedharan, S. Narayanan, Vortex-induced oscillatory response of a circular cylinder due to interference effects, *Journal of Wind Engineering and Industrial Aerodynamics* 49 (1–3) part 1 (1993) 157–166.
[21] B. J. Vickery, A. W. Clark, Lift or across-wind response of tapered stacks, *Journal of the Structures Division* ASCE 98 ST1 (1972) 1–20.
[22] M.M. Zdravkovich, Flow induced oscillations of two interfering circular cylinders, *Journal of Sound and Vibration* 101 (4) (1985) 511–521.